JACS
JOURNAL OF THE AMERICAN CHEMICAL SOCIETY
Article
pubs.acs.org/JACS

Stepwise Two-Photon-Induced Fast Photoswitching via Electron Transfer in Higher Excited States of Photochromic Imidazole Dimer

Yoichi Kobayashi,[†] Tetsuro Katayama,[‡] Takuya Yamane,[†] Kenji Setoura,[‡] Syoji Ito,[‡] Hiroshi Miyasaka,*[,‡] and Jiro Abe*[,†]

[†]Department of Chemistry, School of Science and Engineering, Aoyama Gakuin University, 5-10-1 Fuchinobe, Chuo-ku, Sagamihara, Kanagawa 252-5258, Japan

[‡]Division of Frontier Materials Science and Center for Promotion of Advanced Interdisciplinary Research, Graduate School of Engineering Science, Osaka University, Toyonaka, Osaka 560-8531, Japan

Supporting Information

ABSTRACT: Stepwise two-photon excitations have been attracting much interest because of their much lower power thresholds compared with simultaneous two-photon processes and because some stepwise two-photon processes can be initiated by a weak incoherent excitation light source. Here we apply stepwise two-photon optical processes to the photochromic bridged imidazole dimer, whose solution instantly changes color upon UV irradiation and quickly reverts to the initial color thermally at room temperature. We synthesized a zinc tetraphenylporphyrin (ZnTPP)-substituted bridged imidazole dimer, and wide ranges of time-resolved spectroscopic studies revealed that a ZnTPP-linked bridged imidazole dimer shows efficient visible stepwise two-photon-induced photochromic reactions upon excitation at the porphyrin moiety. The fast photoswitching property combined with stepwise two-photon processes is important not only for the potential for novel photochromic materials that are sensitive to the incident light intensity but also for fundamental photochemistry using higher excited states.

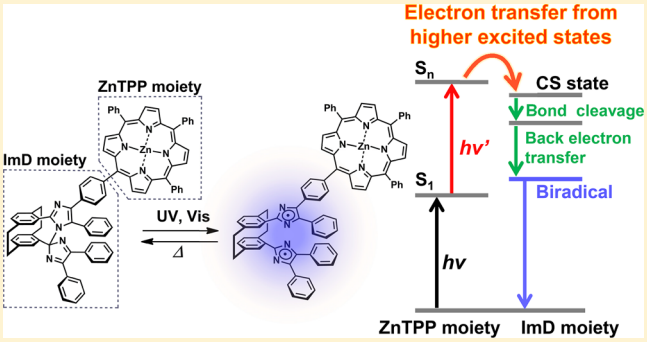

INTRODUCTION

Multiphoton processes in molecular systems can induce specific responses that are usually unattainable by one-photon absorption. The nonlinear dependence of the multiphoton process on the light intensity allows the confinement of the photoresponse in a tiny space, whose property has been utilized in two-photon microscopy,[1,2] three-dimensional lithographic fabrication of microdevices,[3,4] optical storage,[5] and so forth. For the excitation of molecules, simultaneous and sequential multiphoton absorption processes are among the typical methods to induce photochemical reactions. The excited state produced by the two-photon absorption is, in principle, a forbidden state inaccessible by a one-photon allowed transition, and the high energy level of the excited state can be produced especially in sequential two-photon absorption, where the intermediate state produced by the resonant first photon absorption is pumped by the sequential second photon absorption. These features of two-photon excitation lead to specific photochemical responses in various systems.[6−9] One of the present authors (H.M.) and co-workers have applied sequential two-photon excitation to photochromic systems[10] and found that the conversion efficiency of the ring-opening reactions in photochromic diarylethene[10−17] and fulgide[18,19] derivatives can be enhanced from more than tens of times to thousands of times compared with that in the one-photon process. This gating of the reaction by the light intensity can open new functions such as compatibility of photoreadable and photoerasable memory systems and one-color control of both directions of photochromic reactions.[17]

Multiphoton processes have also been found in molecular aggregates. Masuhara and co-workers have reported that the photochemical reaction of spironaphthooxazine crystal, which is not induced under steady-state light irradiation, can take place with a power threshold under femtosecond pulsed laser excitation.[20−22] The nonlinearity of the reaction is due to the cooperative response in the reactions with the large geometrical change in the molecules. That is, the photochemical reaction with the large geometrical change is prohibited in the rigid lattice environment in the case where only a small number of molecules are excited. On the other hand, producing a large number of excited molecules at the same time in the small space allows the geometrical change in the rigid crystal to occur through the cooperative response. Similar cooperative responses of photoisomerization reactions have also been reported for H-aggregates of azobenzene derivatives.[23]

Although these several studies have opened specific photoresponses through multiphoton processes, most of these

Received: February 9, 2016
Published: April 18, 2016

DOI: 10.1021/jacs.6b01470
J. Am. Chem. Soc. 2016, 138, 5930−5938

reactions are based on the intramolecular photochemical process of a single chromophore, and there have been few reports on multiphoton induced intermolecular reactions between two or more chromophores. This is mainly due to the short lifetime of the highly electronically excited state, which is typically less than 1 ps. Multiphoton-induced intermolecular or interchromophore photochemical reactions with high rate constants, however, can extend the new photochemical responses in general, leading to novel photochemistry that overcomes Kasha's rule and advanced photofunctional materials.

Here, to realize a novel photofunctional material using higher excited states, we developed a fast photoswitch compound, zinc tetraphenylporphyrin (ZnTPP)-linked bridged imidazole dimer (compound **1** in Scheme 1). The bridged imidazole dimer

Scheme 1. Photochromic Reaction Scheme of ZnTPP-Linked Bridged Imidazole Dimer (ImD−ZnTPP, 1)

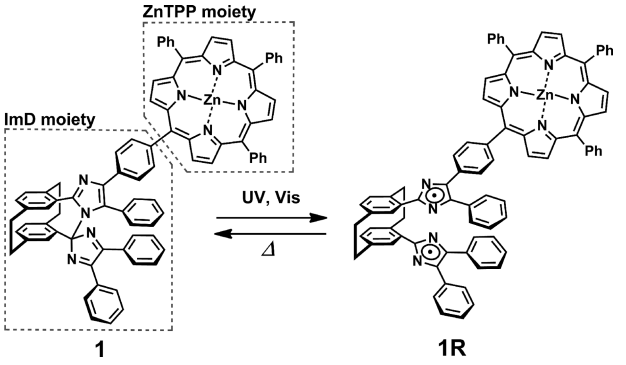

moiety, which was previously named *pseudogem*-bisDPI[2.2]-PC,[24] is abbreviated as ImD for simplicity. ImD is one of the fast T-type photoswitch molecules, which changes the solution color upon UV light irradiation, while the color quickly fades once UV light irradiation stops.[24−27] The ZnTPP moiety of **1** acts as a visible-light harvesting unit because of its high absorption coefficient in the visible region. While UV light induces the photochromism of **1** by a one-photon process, visible light at around 550 nm induces the photochromism by stepwise two-photon processes involving electron transfer from the higher excited state of ZnTPP to ImD, as shown in Figure 1. These photochromic reactions of **1** are revealed by transient absorption spectroscopy over a wide time range of picoseconds to hundreds of milliseconds. In addition to the importance for

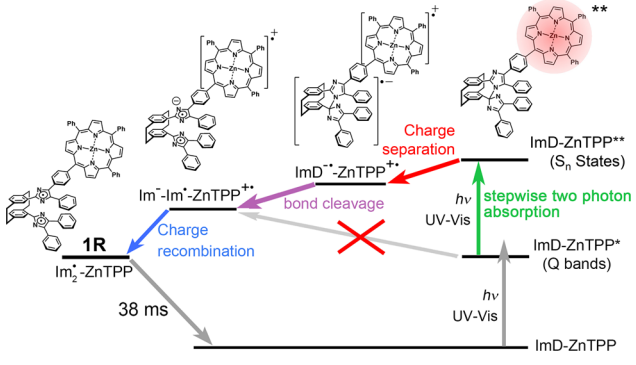

Figure 1. Plausible photochromic reaction pathway of **1** upon excitation with visible light.

fundamental photochemistry, the combination of fast photoswitch properties and nonlinear optical effects would open up novel applications of photochromic materials whose photochromic reactions are altered depending on the incident light intensity.

RESULTS AND DISCUSSION

Figure 2 shows steady-state absorption spectra of ZnTPP, ImD, and ImD−ZnTPP (**1**). Strong absorption peaks at 423 and 548

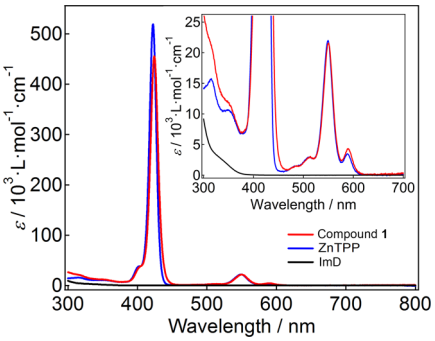

Figure 2. Steady-state absorption spectra of **1**, ZnTPP, and ImD in benzene at room temperature. The ordinate is expanded in the inset.

nm and weak absorption peaks at 589, 511, and 483 nm for ZnTPP are assigned to the Soret band and Q bands, respectively. On the other hand, the absorption of ImD gradually increases at wavelengths shorter than 400 nm, with much smaller absorption coefficients than for ZnTPP (Figure 2 inset). Compared with the untethered system, the relative intensities of the Q band at around 590 nm and the absorption tail of the Soret band at around 450−470 nm for **1** are slightly larger. However, the absorption peaks and band shapes in the tethered system are almost reproduced by the superposition of those of untethered ImD and ZnTPP, indicating that the electronic interaction between the ZnTPP and ImD moieties is small in the ground state. Because the ImD moiety has absorption bands only in the UV wavelength region, the irradiation in the visible region corresponds to selective excitation of the ZnTPP moiety in **1**.

Figure 3a shows picosecond transient absorption spectra of **1** in benzene solution (4.6×10^{-5} M) excited with a 532 nm picosecond laser pulse with a fluence of 0.06 mJ mm^{-2}. A strong absorption band at around 445 nm and dip signals at 544, 586, and 645 nm appear within the response of the apparatus. These dip signals are due to bleaching of the Q band at 548 nm, stimulated emission at 645 nm, and a mixture of these two contributions at 589 nm, which are attributable to the $S_n \leftarrow S_1$ absorption spectrum of the ZnTPP moiety because the $T_n \leftarrow T_1$ absorption spectrum of ZnTPP does not have a dip due to stimulated emission (Figure S10).[28] The spectral band shape evolves over several nanoseconds, and a new absorption band at 840 nm, which is due to the T_1 state of the ZnTPP moiety, is observed at 6 ns. The time constant of the spectral evolution is 2.0 ns, which is almost the same as the fluorescence lifetime of free ZnTPP (Figure S11). That is, no effective quenching of the ZnTPP moiety took place in **1** in the fluorescent state, and the dynamics of the ZnTPP moiety in the S_1 state is independent of the ImD moiety.

Figure 3b shows the transient absorption spectrum of **1** in benzene solution with a fluence of 1.2 mJ mm^{-2}. The spectral band shape immediately after the excitation (e.g., at 20 ps) is

DOI: 10.1021/jacs.6b01470
J. Am. Chem. Soc. 2016, 138, 5930−5938

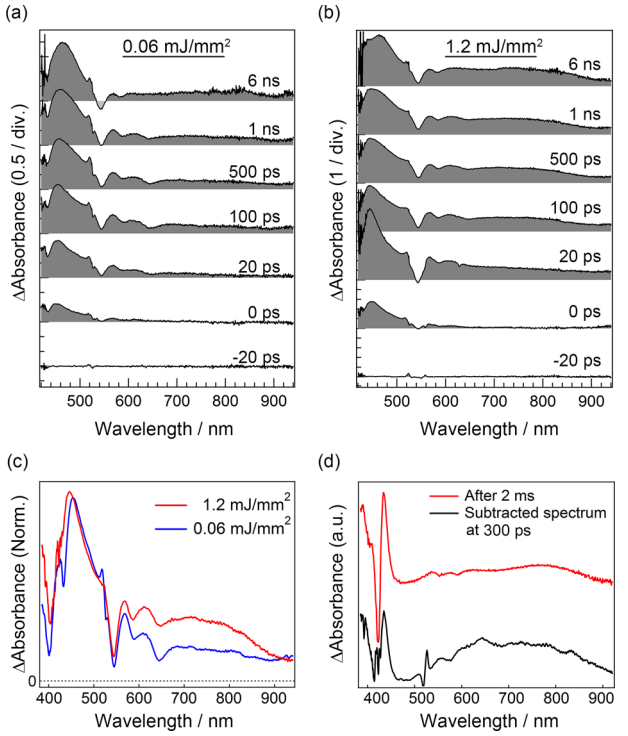

Figure 3. (a, b) Transient absorption spectra of **1** in degassed benzene (4.6×10^{-5} M) excited with a 532 nm picosecond laser pulse at (a) low (0.06 mJ mm^{-2}) and (b) high (1.2 mJ mm^{-2}) pump power. (c) Normalized transient absorption spectra of **1** excited at low (blue line) and high (red line) pump powers at 300 ps. (d) Difference spectrum obtained from the transient absorption spectra excited at low and high pump intensities at 300 ps. The transient spectrum of **1** at 2 ms time delay excited with a nanosecond laser pulse is also shown as a red line.

obviously different from that excited with the lower excitation intensity shown in Figure 3a. Within 100 ps after the excitation, the sharp absorption at around 450 nm decreases, and a broad absorption band appears in the wavelength region >600 nm. To elucidate the transient species produced under the higher-excitation conditions, the absorption spectrum of this new species was obtained by subtracting the contribution from the $S_n \leftarrow S_1$ transition of the ZnTPP moiety in the following manner. As shown in Figure 3a, the S_1 state of the ZnTPP moiety undergoes intersystem crossing to yield the T_1 state with a time constant of 2.0 ns. The absorption coefficient of the $T_n \leftarrow T_1$ transition of ZnTPP at 460 nm was reported to be quite large (74 000 cm^{-1} mol^{-1}).[29] Hence, the absorption spectra at 6 ns after the excitations under the two different excitation conditions were normalized at 460 nm. The multiplying factor for the lower-excitation conditions obtained at 6 ns, 1.58, was used for the subtraction of the spectrum at each of the delay times. The normalized absorption spectra at 300 ps and the difference spectrum thus obtained are shown in Figure 3c,d, respectively. This difference spectrum at 300 ps (Figure 3d) is similar to that of the imidazolyl radical pair (**1R**) observed 2 ms after excitation of ImD in benzene solution with a nanosecond laser pulse at 355 nm.[24] This result shows that **1R** is produced in **1** under the higher-excitation conditions with a 532 nm picosecond laser pulse, although the formation of the radical pair was not observed under the lower-excitation conditions. This result clearly indicates that some nonlinear process is responsible for the production of the radical pair in **1**.

To precisely elucidate this nonlinear process, the transient absorbance at 770 ± 30 nm, at which the radical pair **1R** has large contribution, was plotted as a function of the excitation intensity at 532 nm (Figure 4). The monitoring delay time was

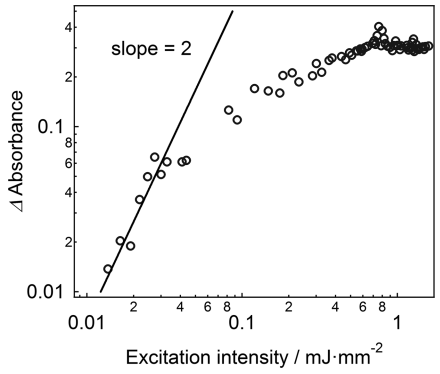

Figure 4. Pump power dependence of the logarithmic transient absorption signal of **1** in degassed benzene (4.6×10^{-5} M) excited at 532 nm and probed at 770 nm. The slope of the straight line is 2.

300 ps, and both axes are given in logarithmic scales. In the low-pump-power regime, the transient signal quadratically increases with an increase in the excitation intensity, as shown by the straight line in Figure 4 (the slope is 2). This result indicates that the two-photon process is responsible for the nonlinear formation of **1R**. With further increases in the excitation intensity, the saturation tendency of the signal intensity is pronounced, probably as a result of the decrease in the population of the ground state. In actuality, the number of photons in the exposed volume is almost the same as the number of **1** molecules. That is, the number of photons at the excitation intensity of 0.5 mJ mm^{-2} corresponds to 1.32×10^{20} photons L^{-1} or 2.2×10^{-4} M, which is much larger than the concentration of the solute (4.6×10^{-5} M). Previously, the effect of the depletion of the ground-state molecules and the inner filter effect of ZnTPP were analyzed as functions of the laser pulse energy, concentration of the ground state, absorption coefficient, and pulse duration.[30,31] By comparing the present result to those of the previous reports, we find that almost all of the molecules in the ground state can be pumped up into the excited state under the present conditions, leading to the saturation behavior in the excitation intensity dependence of the transient absorbance. In any event, the nonlinear dependence of the spectral band shape on the excitation intensity, together with the quadratically increasing transient absorbance, indicates that the two-photon process is responsible for the appearance of the imidazolyl radical in **1**.

Under the present condition of the excitation intensity, the most probable mechanism for the biphotonic process is two-photon absorption by the solute molecule. Generally, two-photon absorption can be classified into two cases: the simultaneous process and the stepwise process.[32] The simultaneous two-photon absorption process occurs through a virtual state, while the stepwise process occurs via an actual transient state such as an excited state. For the simultaneous process, the number of molecules excited by the two-photon absorption, N_e, is represented by eq 1:

$$N_e = N_g \sigma_2 I^2 \quad (1)$$

DOI: 10.1021/jacs.6b01470
J. Am. Chem. Soc. 2016, 138, 5930−5938

where N_g, σ_2, and I are the number of molecules in the ground state, the two-photon absorption cross section, and the light intensity, respectively. The 1 mJ mm^{-2} output of the picosecond laser pulse at 532 nm with a full width at half-maximum (fwhm) of 15 ps corresponds to $I = 1.79 \times 10^{28}$ photons cm^{-2} s^{-1}. The value of N_g is 6.02×10^{16} molecules cm^{-3} for a concentration of 1×10^{-4} M. With the typical value of the two-photon absorption cross section of porphyrin systems,[33,34] 10^{-47} to 10^{-50} cm^4 s photon^{-1} molecule^{-1} (1–1000 GM), the number of excited-state molecules produced by the above I value is estimated to be 2.87×10^{12}–10^{15} molecules cm^{-3} or 4.78×10^{-9}–10^{-6} M. This estimation indicates that the simultaneous two-photon process is negligible under the present excitation conditions. In actuality, no formation of radicals or other transient species was observed for the 550 nm excitation of unsubstituted ImD. These results indicate that the stepwise two-photon absorption process leading to the formation of the higher excited state of the ZnTPP moiety in **1** leads to the production of **1R** and that the simultaneous two-photon absorption is rather difficult for the present excitation conditions of the picosecond laser pulse.

Although the above results indicate that stepwise two-photon absorption leads to the production of **1R**, the mechanism and the intermediate state have not yet been clarified. Figure 5

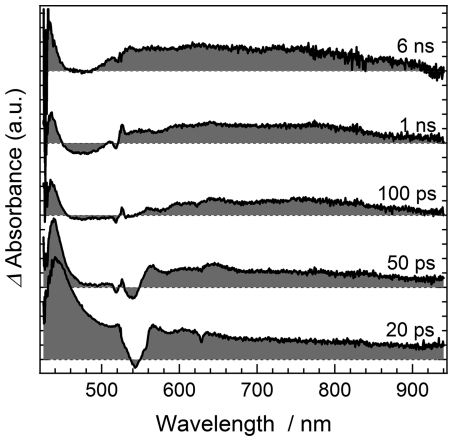

Figure 5. Time evolution of the difference spectrum obtained by subtracting 1.58 times the transient absorption spectrum of **1** in degassed benzene (4.6×10^{-5} M) excited at low pump intensity from the transient absorption spectrum excited at high pump intensity.

shows the time evolution of the difference spectra obtained by the above procedure. The spectrum in the early stage after the excitation evolves into a rather broad one in the time region <100 ps. At and after ca. 100 ps, the spectral band shape gradually evolves. This might be due to insufficient subtraction of the contribution from the one-photon process (S_1 to T_1 of the ZnTPP moiety). Hence, we concentrate on the difference absorption spectra in the early stage after the excitation, showing the quite different band shape. The most striking difference is a strong peak at 460 nm and broad absorption over the visible region. The spectral band shape is close to that of the cation radical of the ZnTPP moiety.[35,36] However, spectra of the transient species of porphyrin derivatives are similar to one another. Hence, to more clearly confirm the contribution of the cation, we measured the absorption spectrum of the cation radical of ZnTPP (ZnTPP$^{+\bullet}$) produced by the electron transfer reaction with methyl viologen (MV^{2+}).

Figure 6 shows transient absorption spectra of ZnTPP with MV^{2+} (70 mM) in methanol/acetone (1:1) binary solution. To

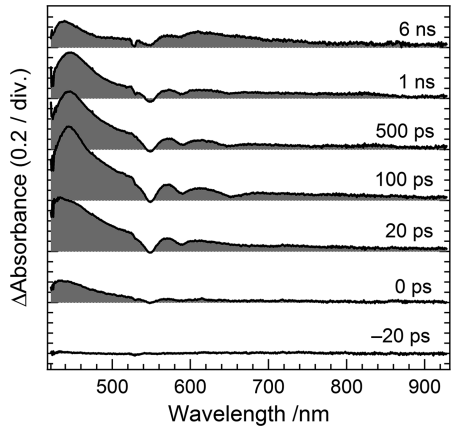

Figure 6. Transient absorption spectra of ZnTPP (1.2×10^{-4} M) with MV^{2+} (70 mM) in methanol/acetone (1:1) binary solution upon excitation with a 532 nm picosecond laser pulse.

increase the concentration of MV^{2+}, we used this binary solution. In this solution, almost 70% of the fluorescence from ZnTPP is quenched. The absorption spectrum immediately after the excitation, which is safely ascribable to the $S_n \leftarrow S_1$ transition, gradually evolves in time into the new spectrum due to the charge-separated (CS) state of ZnTPP$^{+\bullet}$ and methyl viologen monocation (MV^+). Because MV^{2+} quenches both singlet and triplet excited states[37] with rate constants close to the diffusion-limited one, the transient absorption spectrum at 6 ns is mainly composed of the CS state.

Figure 7a shows the transient absorption spectrum (blue line) of ZnTPP with MV^{2+} in methanol/acetone (1:1) binary solution at 6 ns after excitation with a 532 nm picosecond laser pulse together with the difference spectrum (red line) obtained by subtracting 1.58 times the transient absorption spectrum of **1** in benzene solution at 20 ps after 532 nm picosecond laser excitation with a fluence of 0.06 mJ mm^{-2} from the spectrum of **1** at 20 ps after excitation with a fluence of 1.2 mJ mm^{-2} to exclude the contribution of the $S_n \leftarrow S_1$ transition. The two spectra are normalized at 440 nm. As shown in this figure, although a difference in spectral band shape is observed in the wavelength region of 500–750 nm, similar band shapes are confirmed in the shorter-wavelength region. Figure 7b shows the difference spectrum obtained from the transient absorption spectrum of **1** observed at 20 ps after excitation and that of ZnTPP with MV^{2+} observed at 6 ns after excitation. By comparing the difference spectrum in Figure 7b with the reference absorption spectrum of MV^+ in Figure 7c,[34] one can see that the spectral band shape and absorption maximum of the difference spectrum are almost the same as those of MV^+. This result clearly indicates that the transient absorption spectrum of **1** observed at 20 ps after 532 nm picosecond laser excitation with a fluence of 1.2 mJ mm^{-2} is mainly due to the ZnTPP$^{+\bullet}$ moiety. The previous report revealed that the anion radical of ImD (ImD$^{-\bullet}$) generated by electrochemical reduction has no strong absorption band in the visible region.[39] Hence, the transient absorption spectrum of **1** shown in Figure 7a mainly comprises peaks due to the ZnTPP$^{+\bullet}$ moiety even though the ImD$^{-\bullet}$ moiety is produced by the charge separation between the ZnTPP and ImD moieties. Actually, the cation radical of unsubstituted ZnTPP in benzene solution was not

DOI: 10.1021/jacs.6b01470
J. Am. Chem. Soc. 2016, 138, 5930–5938

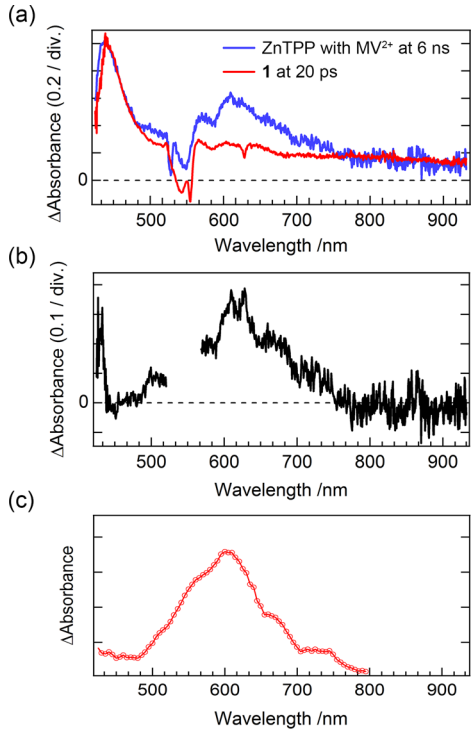

Figure 7. (a) Transient absorption spectrum of ZnTPP with MV^{2+} (70 mM) in methanol/acetone binary solution observed at 6 ns after excitation with a 532 nm picosecond laser pulse (blue line) and the difference spectrum of **1** in benzene solution observed at 20 ps after excitation with a 532 nm picosecond laser pulse (red line). (b) Difference spectrum obtained from the two spectra in (a). (c) Steady-state absorption spectrum of MV^{+} in methanol solution.[38]

observed under the present excitation conditions with high laser intensity. These results indicate that the charge separation takes place between the ZnTPP moiety in the two-photon-accessible higher excited state and the ImD moiety in **1**. The transient species attributable to the CS state of **1** ($ImD^{-\bullet}$–$ZnTPP^{+\bullet}$) decays on the time scale of a few tens of picosecnds, as shown in Figure S12, and the broad absorption of the imidazolyl radical pair moiety appears with this decay. Accordingly, the decay of the CS state leads to the formation of **1R**.

Charge separation between the Zn porphyrin in the excited state and the electron acceptor was systematically studied by Mataga and co-workers using various porphyrin systems in which the electron donor and acceptor were connected by a covalent bond.[40−43] They reported that for the process of charge separation between Zn porphyrin in the S_2 state and electron acceptors directly attached to the porphyrin in toluene solution, the charge separation rate constant showed the maximum value (7×10^{12} s^{-1}) at an energy gap, ΔE, of ca. 0.5 eV. In addition, charge separation reaction rate constants larger than 2×10^{12} s^{-1} were observed in the region where ΔE is between 0.0 and 1.0 eV.

The energy level of the CS state between the ZnTPP and ImD moieties could be estimated using the conventional equation based on the oxidation and reduction potentials and the Born equation for the correction of the solvent, and a value of 2.82 eV was obtained (see the SI). The high excited state of the ZnTPP moiety of **1** attained by the successive two-photon absorption is estimated to be ca. 4.4 eV. (The two-photon energy at 532 nm corresponds to 4.66 eV. The energy of the relaxed S_1 state of the ZnTPP moiety is 2.07 eV. In the case that the absorption of the second photon takes place at the relaxed S_1 state of the ZnTPP moiety, the excited state at 4.4 eV will be produced.) The energy level of the lowest excited state of the ImD moiety of **1** could be estimated to be ca. 400 nm (3.1 eV).[44] That is, the energy level of the CS state is lower than the high excited state of the ZnTPP moiety attained by the two-photon absorption and much higher than the S_1 state of the ZnTPP moiety. Because the rapid relaxation may take place from the high excited state of the ZnTPP moiety in **1**, the energy gap for the CS process is difficult to estimate explicitly. However, a fast CS process comparable with the relaxation into the S_1 state (typically on the order of 10^{-13} s) could be expected judging from the energy-gap dependence reported by Mataga and co-workers.[45]

The two-photon-induced photochromic reaction can be initiated with a nanosecond laser pulse as well as a picosecond laser source. In Figure 8 we show the transient absorption

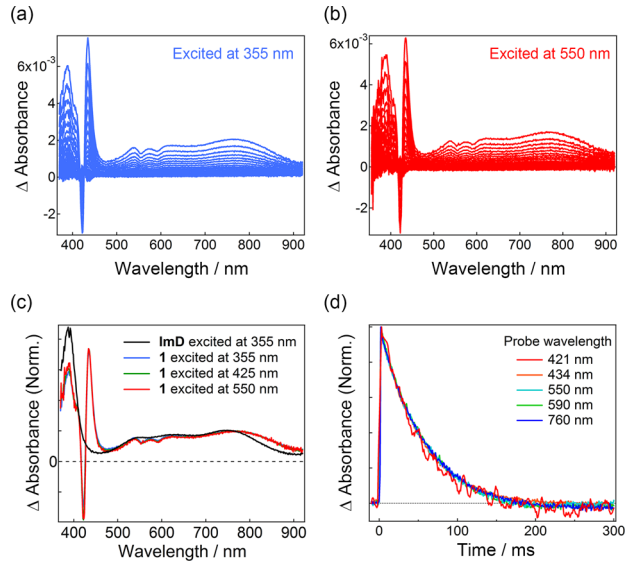

Figure 8. Transient absorption spectra of **1** in degassed benzene at 297 K (1.6×10^{-6} M) excited with (a) 355 and (b) 550 nm nanosecond laser pulses. (c) Normalized transient absorption spectra of **1** excited at 355, 425, and 550 nm and ImD excited at 355 nm at 20 ms. (d) Normalized transient absorption dynamics of **1** probed at different wavelengths after excitation at 550 nm.

spectra of **1** in benzene solution (1.6×10^{-6} M) upon excitation with a 355 nm nanosecond laser pulse (5 ns fwhm and 0.11 mJ mm^{-2} output power) and those excited with a 550 nm nanosecond laser pulse (0.15 mJ mm^{-2}). As Figure 8a,b show, almost the same spectra and time evolution were observed under these two sets of excitation conditions. Figure 8c shows normalized transient absorption spectra of **1** at 20 ms after excitation with laser pulses at 355, 425, and 550 nm, together with the transient absorption spectrum of ImD observed at 20 ms after excitation with a 355 nm nanosecond laser pulse. This figure confirms again that **1R** is produced even by excitation of the ZnTPP moiety.

Figure 8d shows normalized time profiles of the transient absorbance of **1** monitored at different wavelengths following excitation at 550 nm. All of the time profiles show first-order decay to the baseline with a half-life of 38 ms. In addition, the steady-state absorption after the photolysis was the same as that

DOI: 10.1021/jacs.6b01470
J. Am. Chem. Soc. 2016, 138, 5930−5938

before the photoirradiation. These results indicate that this first-order decay is ascribable to recombination in **1R** returning to the parent molecule **1**. The time profiles of the transient absorption signals of **1** excited at 355 and 425 nm were identical to that for excitation at 550 nm, while the amplitudes were different (Figure 9), as will be discussed later. The half-life

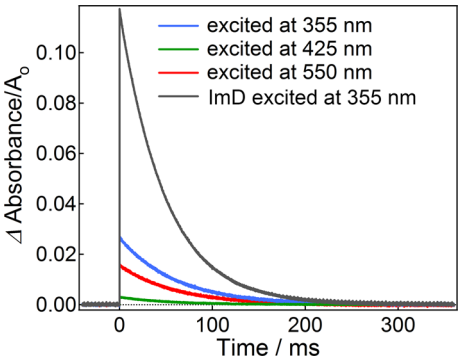

Figure 9. Transient absorption dynamics of **1** excited at different excitation wavelengths (355, 425, and 550 nm) and that of ImD (excited at 355 nm). The transient absorption signals were divided by A_0.

of the thermal back-reaction of **1R** (38 ms) is almost the same as that of ImD (33 ms).[24] In addition, it should be noted that a bleach signal due to the Soret band of the ZnTPP moiety at 421 nm and the positive sharp signal near the bleach (433 nm) indicate that the Soret band of the ZnTPP moiety is affected by the imidazolyl radical pair moiety. It is noteworthy that the spectral shape does not change at all with time, as shown in Figure S11, and that the ZnTPP moiety has already relaxed to the ground states on this time scale. These results indicate that no intermediates are formed on this time scale.

The temperature dependence of the transient absorption dynamics of **1** excited and probed at 355 and 760 nm, respectively, was analyzed to reveal the thermodynamic parameters ($\Delta H^{\ddagger}$, $\Delta S^{\ddagger}$, $\Delta G^{\ddagger}$) using Eyring plots (Table 1 and Figure S15). This analysis showed that all of the thermodynamic parameters are very similar to those of unsubstituted ImD[24] and that the thermal back-reaction process of **1R** is little affected by the ZnTPP moiety. The similar thermodynamic parameters of **1** and ImD again confirm that the ZnTPP moiety relaxes to the ground state.

The excitation intensity dependence of the transient absorbance of **1** due to **1R** with a 550 nm nanosecond laser pulse (probed at 760 nm 0.4 ms after excitation) is shown in Figure S16. The nonlinear formation of **1R** was also confirmed in the nanosecond photolysis.

We further investigated the relative efficiency of the two-photon-induced photochromic reaction of **1** at different excitation wavelengths. ImD was used as a standard sample because it induces only the one-photon process and its molecular backbone is included in **1**. We assumed that the absorption coefficients of the transient species of **1** and ImD were the same. The absorbance at the excitation wavelength of the steady-state absorption spectra (A_0) was set to be the same (0.66−0.67) under all of the excitation conditions by changing the concentrations in order to avoid experimental artifacts. Figure 9 shows the transient absorption dynamics of **1** and ImD upon excitation with nanosecond laser pulses having different wavelengths (excitation wavelength = 355 nm, pulse width = 5 ns, and energy density = 0.44 mJ mm^{-2}). The probe wavelength was set to 760 nm. The figure clearly shows that the signal amplitude of **1** was smaller than that of ImD excited at 355 nm but is large for the two-photon process. By comparing the maximum signal amplitudes divided by A_0, we estimated the relative efficiencies for the two-photon-induced photochromic reactions. Compared with the efficiency of the one-photon-induced photochromic reaction of ImD, the relative efficiencies of the photochromic reaction of **1** upon excition at the Q band (550 nm) and the Soret band (425 nm) of the ZnTPP moiety are estimated to be 14% and 2.7%, respectively. The relative efficiency of **1** upon excitation at 355 nm is similar to that upon excitation at 550 nm. It should be noted that these efficiencies are not the quantum efficiencies for these photochromic reactions but simply the relative efficiencies compared with the efficiency of the one-photon-induced photochromic reaction. The efficiency upon excitation at 425 nm is obviously smaller than those for excitation at 355 and 550 nm. While there have been several reports of charge transfer from the Soret band to other compounds,[40−42] this result suggests that the Soret band of the ZnTPP moiety in **1** is not involved in the stepwise two-photon-gated photochromic reaction. Upon excitation of the Soret band, the two-photon process probably occurs from the Q band after relaxation from the Soret band to the Q band.

CONCLUSION

The photochromic reaction scheme of **1** via the stepwise two-photon process is summarized in Figure 1. First, the photon energy absorbed by the ZnTPP moiety relaxes to the S_1 state. Second, under the high excitation intensity, the ZnTPP moiety absorbs an additional photon, and the transition from the S_1 state to the S_n state occurs. Third, the electron of the ZnTPP moiety is transferred to the ImD moiety, which results in the CS state ($ImD^{-\bullet}$−$ZnTPP^{+\bullet}$). This CS state disappears within 100 ps. Because the energy level of the CS state was estimated to be lower than the S_1 level of the ImD moiety, $Im^{\bullet}_2$−ZnTPP (**1R**) is produced by the other route. It is worth noting that $Im^{\bullet}_2$−ZnTPP could be produced by bond cleavage in the CS state because a previous electrochemical study showed that the injection of an electron to ImD cleaves the C−N bond to produce the imidazolyl radical and the imidazole anion. Accordingly, the C−N bond of $ImD^{-\bullet}$−$ZnTPP^{+\bullet}$ may be spontaneously cleaved to form Im^{-}−$Im^{\bullet}$−$ZnTPP^{+\bullet}$, and the subsequent charge recombination process leads to $Im^{\bullet}_2$−ZnTPP.

The radical pair is the origin of the photocoloration, and the color fades with a half-life of 38 ms by the thermal back-

Table 1. Activation Parameters for the Thermal Back-Reaction from the Colored Form to the Colorless Form for 1 and ImD at 298 K

	$\Delta H^{\ddagger}$/kJ mol^{-1}	$\Delta S^{\ddagger}$/kJ mol^{-1} K^{-1}	$\Delta G^{\ddagger}$/kJ mol^{-1}	k/s^{-1}	$\tau_{1/2}$/ms
1	59.7	−20.5	65.8	18	38
ImD	58.8	−22.2	65.5	21	33

DOI: 10.1021/jacs.6b01470
J. Am. Chem. Soc. 2016, 138, 5930−5938

reaction to recover **1**. Notably, one-photon excitation of the ZnTPP moiety does not contribute to the photochromic reaction of **1**. Moreover, the relative efficiency of the two-photon-induced photochromic reaction is relatively high compared with reported two-photon absorption systems, and this two-photon-induced photochromism can be initiated even by a weak nanosecond laser pulse. The present result is the first example of a two-photon-sensitized photochemical reaction realizing fast photoswitching in materials, and this system would be important for novel functional materials using higher excited states.

EXPERIMENTAL SECTION

Synthesis. All of the reactions were monitored by thin-layer chromatography carried out on 0.2 mm E. Merck silica gel plates (60 F_{254}). Column chromatography was performed on silica gel (Wakogel C-300). All of the reagents and solvents were obtained from commercial suppliers (Sigma-Aldrich, Wako Chemicals, TCI, Acros Organics) and used without further purification. All of the reaction solvents were distilled on the appropriate drying reagents prior to use. Compound **1** was prepared as shown in Scheme 2.

Scheme 2. Synthetic Procedure for 1

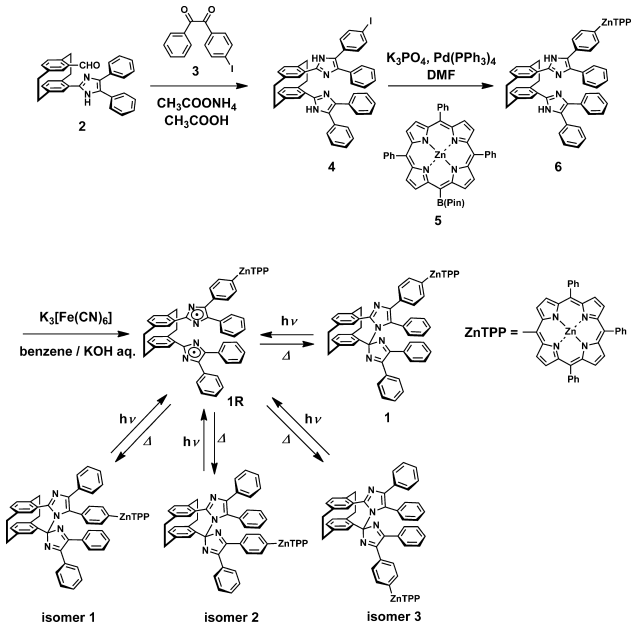

*pseudogem-[4-Formyl-13-(4,5-diphenyl-1H-imidazol-2-yl)][2.2]-paracyclophane (**2**).* Compound **2** was prepared according to a literature procedure.[46]

*1-(4-Iodophenyl)-2-phenylethane-1,2-dione (**3**).* Compound **3** was prepared according to a literature procedure.[47]

*pseudogem-[4-(4-(4-Iodophenyl)-5-phenyl-1H-imidazol-2-yl)-13-(4,5-diphenyl-1H-imidazol-2-yl)][2.2]paracyclophane (**4**).* A solution of **2** (57.9 mg, 0.127 mmol), **3** (51.2 mg, 0.152 mmol), and ammonium acetate (287 mg, 3.72 mmol) in acetic acid (1.5 mL) was stirred for 12 h at 110 °C. The reaction mixture was allowed to cool to room temperature, and the mixture was neutralized with aqueous ammonia. The crude product was washed with dichloromethane to give **4** as a pale-yellow solid (93.0 mg, 95% yield) as mixture of two structural isomers. ^{1}H NMR (400 MHz, DMSO-d_6): δ 11.95 (s, 1H), 11.76 (s, 1H), 11.65 (m, 2H), 7.46 (d, J = 8.4 Hz, 1H), 7.39−7.34 (m, 5H), 7.28−7.01 (m, 35H), 6.84 (d, J = 8.3 Hz, 1H), 6.71 (d, J = 7.7 Hz, 4H), 6.62 (d, J = 7.7 Hz, 4H), 4.59−4.49 (m, 4H), 3.15−3.05 (m, 12H). HR-ESI-TOF-MS (m/z): calcd 771.1979 ($C_{46}H_{36}IN_4$); found 771.1959 $[M + H]^+$.

*[5-(4,4,5,5-Tetramethyl-{1,3,2}dioxaborolan-2-yl)-10,15,20-triphenylporphyrinato]zinc(II) (**5**).* Compound **5** was prepared according to a literature procedure.[48]

*pseudogem-[4-(4-(10,15,20-Triphenyl-21H,23H-porphinezinc)-5-phenyl-1H-imidazol-2-yl)-13-(4,5-diphenyl-1H-imidazol-2-yl)][2.2]-paracyclophane (**6**).* Compounds **4** (40.3 mg, 52.3 μmol) and **5** (35.3 mg, 48.5 μmol) dissolved in DMF (2.0 mL) were mixed with aqueous 1.0 M tripotassium phosphate, and the mixture was purged with N_2 gas. Tetrakis(triphenylphosphine)palladium(0) (3 mg, 2.59 μmol) was added, and the resulting solution was stirred at 80 °C for 12 h. The mixture was extracted with ethyl acetate. The organic layer was dried over Na_2SO_4, filtered, and evaporated. The product was purified by silica gel column chromatography (2:1 hexane/tetrahydrofuran) to give **6** as a purple solid (30.9 mg, 51% yield) as a mixture of two structural isomers. There are four possible structural isomers depending on which nitrogens have hydrogen atoms in the two imidazole rings. However, only two structural isomers were observed in NMR spectra, probably because of rotation of the imidazole rings or negligible differences in the chemical shifts. ^{1}H NMR (400 MHz, DMSO-d_6): δ 12.03 (s, 1H), 11.82 (s, 1H), 11.80 (s, 1H), 11.77 (s, 1H), 8.85−8.77 (m, 17H), 8.22−8.18 (m, 12H), 7.95 (d, J = 7.9 Hz, 2H), 7.88−7.82 (m, 22H), 7.75 (d, J = 8.3 Hz, 2H), 7.56−7.50 (m, 6H), 7.44 (d, J = 7.1 Hz, 2H), 7.33−7.29 (m, 4H), 7.25−7.08 (m, 20H), 7.02 (t, J = 7.4 Hz, 1H), 6.80−6.75 (m, 4H), 6.70−6.65 (m, 4H), 4.82−4.66 (m, 4H), 3.17−3.12 (m, 12H); HR-ESI-TOF-MS (m/z): calcd 1243.4149 ($C_{84}H_{59}N_8Zn$); found 1243.4184 $[M + H]^+$.

*Compound **1**.* A solution of potassium ferricyanide (496 mg, 1.51 mmol) and KOH (153 mg, 2.73 mmol) in water (10 mL) was purged with N_2 gas and then added to a solution of **6** (34.1 mg, 2.7×10^{-2} μmol) in benzene (10 mL) purged with N_2 gas. After 2 h of stirring at room temperature, the resultant mixture was then extracted with benzene. The organic layer was dried over Na_2SO_4, filtered, and evaporated. The product was purified by silica gel column chromatography (3:2 hexane/tetrahydrofuran) to give a purple solid as a mixture of four structural isomers (27.0 mg, 79% yield). One of the four structural isomers (**1**) was separated from the others by high-performance liquid chromatography (3:1 methanol/CH_3CN). ^{1}H NMR (400 MHz, DMSO-d_6): δ 8.23 (d, J = 6.9 Hz, 8H), 8.17−8.14 (m, 6H), 7.90 (d, J = 8.3 Hz, 2H), 7.79−7.78 (m, 9H), 7.69 (d, J = 7.50 Hz, 1H), 7.61 (d, J = 8.3 Hz, 2H), 7.57 (d, J = 7.5 Hz, 1H), 7.47 (t, J = 7.7 Hz, 3H), 7.40−7.23 (m, 9H), 7.07 (d, J = 7.5 Hz, 2H), 6.93 (s, 1H), 6.79−6.74 (m, 2H), 6.60 (d, J = 7.9 Hz, 1H), 6.55 (d, J = 7.9 Hz, 1H), 4.52−4.59 (m, 1H), 3.09−3.02 (m, 7H); HR-ESI-TOF-MS (m/z): calcd 1241.3992 ($C_{84}H_{57}N_8Zn$); found 1241.3990 $[M + H]^+$.

Steady-State Absorption Measurements. Steady-state absorption spectra were measured on a SHIMADZU UV-3600 Plus spectrophotometer at room temperature, and 1 cm quartz cuvettes were used for the experiments.

Picosecond Transient Absorption Measurements. Picosecond transient absorption spectra were measured using a custom-built mode-locked Nd^{3+}:YAG laser.[31,49,50] The second harmonic (532 nm) with a fwhm of 15 ps was employed as an excitation pulse. A white-light supercontinuum as a probe pulse was generated by focusing the fundamental pulse (1064 nm) into a mixture of D_2O and H_2O (3:1) contained in a cell with an optical length of 10 cm. To avoid anisotropic response of the sample, the supercontinuum was circularly polarized using a quarter-wave plate. The sample was set in a quartz cell with an optical length of 2.0 mm, and the solution was not circulated. The focusing area size of the excitation light was ca. 1.8 mm, the center of which was monitored by the white-light continuum with a diameter of less than 1 mm.[31] The repetition rate of the laser was lower than 0.3 Hz. The signal was detected by two sets of multichannel photodiode array systems (Hamamatsu, MOS multi-channel detector C4351) with a polychromator (Jarrell Ash Corp., Monospec27).

Time-Correlated Single-Photon Counting Measurements. Fluorescence time profiles were measured using a time-correlated single-photon counting (TCSPC) system.[51] The excitation light source was provided by a Ti:sapphire laser (Tsunami, Spectra Physics) coupled with a photonic fiber system. The repetition rate of the

DOI: 10.1021/jacs.6b01470
J. Am. Chem. Soc. 2016, 138, 5930−5938

Ti:sapphire laser (80 MHz, ca. 1 W at 870 nm) was reduced to 8 MHz by an EO modulator (M360-80 and 25D, Conoptics), and the output was guided into the photonic fiber system (SCG-800, Newport) to expand the wavelength range to 520−920 nm. By introducing a bandpass filter, we chose the excitation wavelength to be 546 ± 5 nm. Emission was detected at the magic-angle configuration, and a quartz sample cell with an optical length of 1.0 cm was used. A photomultiplier tube (R3809U-50, Hamamatsu Photonics) with an amplifier (C5594, Hamamatsu Photonics) and a counting board (PicoHarp 300, PicoQuanta) was used for signal detection. A monochromator (Oriel 77250, Newport) was placed in front of the photomultiplier tube. The instrumental response function was estimated by the fwhm of the scattered light from a colloidal solution for the excitation light pulse. In the present measurements, it was ca. 30 ps.

Laser Flash Photolysis Measurements. The laser flash photolysis experiments were carried out with a TSP-2000 time-resolved spectrophotometer (Unisoku). A 10 Hz Q-switched Nd:YAG laser (Continuum Minilite II) with the third harmonic at 355 nm was employed for the excitation light. The probe beam from a halogen lamp (OSRAM HLX64623) was guided with an optical fiber scope to be arranged in an orientation perpendicular to the exciting laser beam. The probe beam was monitored with a photomultiplier tube (Hamamatsu R2949) through a spectrometer (Unisoku MD200). Sample solutions were deaerated by argon bubbling prior to the laser flash photolysis experiments.

■ ASSOCIATED CONTENT

Supporting Information

The Supporting Information is available free of charge on the ACS Publications website at DOI: 10.1021/jacs.6b01470.

Synthesis, ^{1}H NMR and HR-ESI-TOF-MS spectra, HPLC chromatograms, UV−vis absorption spectra, transient absorption measurements, estimation of the CS state between the ZnTPP and ImD moieties, and DFT calculations (PDF)

■ AUTHOR INFORMATION

Corresponding Authors

*miyasaka@chem.es.osaka-u.ac.jp
*jiro_abe@chem.aoyama.ac.jp

Notes

The authors declare no competing financial interest.

■ ACKNOWLEDGMENTS

This work was supported partly by the Core Research for Evolutionary Science and Technology (CREST) Program of the Japan Science and Technology Agency (JST) and Grants-in-Aid for Scientific Research on Innovative Areas "Photosynergetics" (26107002 and 26107010) from MEXT, Japan. Financial assistance for this research was also provided by the MEXT-supported Program for the Strategic Research Foundation at Private Universities, 2013−2017.

■ REFERENCES

(1) König, K. *J. Microsc.* **2000**, *200*, 83.
(2) Helmchen, F.; Denk, W. *Nat. Methods* **2005**, *2*, 932.
(3) Kawata, S.; Sun, H. B.; Tanaka, T.; Takada, K. *Nature* **2001**, *412*, 697.
(4) Cumpston, B. H.; Ananthavel, S. P.; Barlow, S.; Dyer, D. L.; Ehrlich, J. E.; Erskine, L. L.; Heikal, A. A.; Kuebler, S. M.; Lee, I.-Y. S.; McCord-Maughon, D.; Qin, J.; Rockel, H.; Rumi, M.; Wu, X.; Marder, S. R.; Perry, J. W. *Nature* **1999**, *398*, 51.
(5) Kawata, S.; Kawata, Y. *Chem. Rev.* **2000**, *100*, 1777.
(6) Boca, S. C.; Four, M.; Bonne, A.; van der Sanden, B.; Astilean, S.; Baldeck, P. L.; Lemercier, G. *Chem. Commun.* **2009**, 4590.
(7) Ishii, K.; Hoshino, S.; Kobayashi, N. *Inorg. Chem.* **2004**, *43*, 7969.
(8) Ishii, K.; Shiine, M.; Shimizu, Y.; Hoshino, S.; Abe, H.; Sogawa, K.; Kobayashi, N. *J. Phys. Chem. B* **2008**, *112*, 3138.
(9) Ueno, K.; Juodkazis, S.; Shibuya, T.; Yokota, Y.; Mizeikis, V.; Sasaki, K.; Misawa, H. *J. Am. Chem. Soc.* **2008**, *130*, 6928.
(10) Miyasaka, H.; Murakami, M.; Itaya, A.; Guillaumont, D.; Nakamura, S.; Irie, M. *J. Am. Chem. Soc.* **2001**, *123*, 753.
(11) Miyasaka, H.; Murakami, M.; Okada, T.; Nagata, Y.; Itaya, A.; Kobatake, S.; Irie, M. *Chem. Phys. Lett.* **2003**, *371*, 40.
(12) Murakami, M.; Miyasaka, H.; Okada, T.; Kobatake, S.; Irie, M. *J. Am. Chem. Soc.* **2004**, *126*, 14764.
(13) Uchida, K.; Takata, A.; Ryo, S.; Saito, M.; Murakami, M.; Ishibashi, Y.; Miyasaka, H.; Irie, M. *J. Mater. Chem.* **2005**, *15*, 2128.
(14) Ishibashi, Y.; Tani, K.; Miyasaka, H.; Kobatake, S.; Irie, M. *Chem. Phys. Lett.* **2007**, *437*, 243.
(15) Tani, K.; Ishibashi, Y.; Miyasaka, H.; Kobatake, S.; Irie, M. *J. Phys. Chem. C* **2008**, *112*, 11150.
(16) Ishibashi, Y.; Okuno, K.; Ota, C.; Umesato, T.; Katayama, T.; Murakami, M.; Kobatake, S.; Irie, M.; Miyasaka, H. *Photochem. Photobiol. Sci.* **2010**, *9*, 172.
(17) Mori, K.; Ishibashi, Y.; Matsuda, H.; Ito, S.; Nagasawa, Y.; Nakagawa, H.; Uchida, K.; Yokojima, S.; Nakamura, S.; Irie, M.; Miyasaka, H. *J. Am. Chem. Soc.* **2011**, *133*, 2621.
(18) Ishibashi, Y.; Murakami, M.; Miyasaka, H.; Kobatake, S.; Irie, M.; Yokoyama, Y. *J. Phys. Chem. C* **2007**, *111*, 2730.
(19) Belfield, K. D.; Liu, Y.; Negres, R. A.; Fan, M.; Pan, G.; Hagan, D. J.; Hernandez, F. E. *Chem. Mater.* **2002**, *14*, 3663.
(20) Suzuki, M.; Asahi, T.; Masuhara, H. *Phys. Chem. Chem. Phys.* **2002**, *4*, 185.
(21) Asahi, T.; Suzuki, M.; Masuhara, H. *J. Phys. Chem. A* **2002**, *106*, 2335.
(22) Suzuki, M.; Asahi, T.; Masuhara, H. *ChemPhysChem* **2005**, *6*, 2396.
(23) Uchida, K.; Yamaguchi, S.; Yamada, H.; Akazawa, M.; Katayama, T.; Ishibashi, Y.; Miyasaka, H. *Chem. Commun.* **2009**, 4420.
(24) Kishimoto, Y.; Abe, J. *J. Am. Chem. Soc.* **2009**, *131*, 4227.
(25) Shima, K.; Mutoh, K.; Kobayashi, Y.; Abe, J. *J. Am. Chem. Soc.* **2014**, *136*, 3796.
(26) Iwasaki, T.; Kato, T.; Kobayashi, Y.; Abe, J. *Chem. Commun.* **2014**, *50*, 7481.
(27) Yamashita, H.; Abe, J. *Chem. Commun.* **2014**, *50*, 8468.
(28) Masuhara, H.; Ikeda, N.; Miyasaka, H.; Mataga, N. *Bunko Kenkyu* **1982**, *31*, 19.
(29) Pekkarinen, L.; Linschitz, H. *J. Am. Chem. Soc.* **1960**, *82*, 2407.
(30) Miyasaka, H.; Masuhara, H.; Mataga, N. *Laser Chem.* **1983**, *1*, 357.
(31) Murakami, M.; Miyasaka, H.; Okada, T.; Kobatake, S.; Irie, M. *J. Am. Chem. Soc.* **2004**, *126*, 14764.
(32) Mutoh, K.; Nakagawa, Y.; Sakamoto, A.; Kobayashi, Y.; Abe, J. *J. Am. Chem. Soc.* **2015**, *137*, 5674.
(33) Drobizhev, M.; Karotki, A.; Kruk, M.; Rebane, A. *Chem. Phys. Lett.* **2002**, *355*, 175.
(34) Kamada, K. *Proc. SPIE* **2004**, *5516*, 97.
(35) Fajer, J.; Borg, D. C.; Forman, A.; Dolphin, D.; Felton, R. H. *J. Am. Chem. Soc.* **1970**, *92*, 3451.
(36) Wahab, A.; Bhattacharya, M.; Ghosh, S.; Samuelson, A. G.; Das, P. K. *J. Phys. Chem. B* **2008**, *112*, 2842.
(37) Pileni, M. P.; Braun, A. M.; Grätzel, M. *Photochem. Photobiol.* **1980**, *31*, 423.
(38) Peon, J.; Tan, X.; Hoerner, J. D.; Xia, C.; Luk, Y. F.; Kohler, B. *J. Phys. Chem. A* **2001**, *105*, 5768.
(39) Mutoh, K.; Nakano, E.; Abe, J. *J. Phys. Chem. A* **2012**, *116*, 6792.
(40) Mataga, N.; Chosrowjan, H.; Taniguchi, S. *J. Photochem. Photobiol., C* **2005**, *6*, 37.
(41) Mataga, N.; Chosrowjan, H.; Taniguchi, S.; Shibata, Y.; Yoshida, N.; Osuka, A.; Kikuzawa, T.; Okada, T. *J. Phys. Chem. A* **2002**, *106*, 12191.

DOI: 10.1021/jacs.6b01470
J. Am. Chem. Soc. 2016, 138, 5930−5938

(42) Mataga, N.; Miyasaka, H. *Adv. Chem. Phys.* **1999**, *107*, 431.
(43) Mataga, N.; Taniguchi, S.; Chosrowjan, H.; Osuka, A.; Kurotobi, K. *Chem. Phys. Lett.* **2005**, *403*, 163.
(44) Nakano, E.; Mutoh, K.; Kobayashi, Y.; Abe, J. *J. Phys. Chem. A* **2014**, *118*, 2288.
(45) In the case that the relaxation of the electronic state from the highly excited state is faster than the CS process, the relaxation could preferentially take place. However, the energy level of the highly excited state attained by the succesive two-photon absorption (4.4 eV) is higher than the CS level (2.82 eV). Therefore, the CS rate constant could become large during the relaxation of the electronic state.
(46) Harada, Y.; Hatano, S.; Kimoto, A.; Abe, J. *J. Phys. Chem. Lett.* **2010**, *1*, 1112.
(47) Yamashita, K.-I.; Tsuboi, M.; Asano, M. S.; Sugiura, K.-I. *Synth. Commun.* **2012**, *42*, 170.
(48) Finnigan, E. M.; Rein, R.; Solladié, N.; Dahms, K.; Götz, D. C. G.; Bringmann, G.; Senge, M. O. *Tetrahedron* **2011**, *67*, 1126.
(49) Miyasaka, H.; Moriyama, T.; Kotani, S.; Muneyasu, R.; Itaya, A. *Chem. Phys. Lett.* **1994**, *225*, 315.
(50) Miyasaka, H.; Moriyama, T.; Itaya, A. *J. Phys. Chem.* **1996**, *100*, 12609.
(51) Nagasawa, Y.; Oishi, A.; Itoh, T.; Yasuda, M.; Muramatsu, M.; Ishibashi, Y.; Ito, S.; Miyasaka, H. *J. Phys. Chem. C* **2009**, *113*, 11868.

DOI: 10.1021/jacs.6b01470
J. Am. Chem. Soc. 2016, 138, 5930−5938